



RESEARCH AND DESIGN OF GRID-CONNECTED INVERTER IN PHOTOVOLTAIC SYSTEM WITH SVPWM TECHNIQUE

Nguyen Duc Minh ^{*1}, Bui Van Huy ², Ngo Thi Quan ³, Nguyen Quang Ninh ¹, Trinh Trong Chuong ²

¹ Institute of Energy Science - Vietnam Academy of Science and Technology, Vietnam

² Hanoi University of Industry, Vietnam

³ Da Nang University of Science and Technology, Vietnam



Abstract:

This paper presents the design and simulation of three phase grid-connected inverter for photovoltaic systems with power ratings up to 5 kW. In this research, the application of Space Vector Pulse Width Modulation (SVPWM) technique for inverter is explored. With the use of SVPWM inverter, synchronization between the inverter and electrical grid follows the Phase-locked Loop (PLL) algorithm. The proposed design is simulated and validated by experimental results.

Keywords: SVPWM; Reactive Power Control; Solar Energy; PLL.

Cite This Article: Nguyen Duc Minh, Bui Van Huy, Ngo Thi Quan, Nguyen Quang Ninh, and Trinh Trong Chuong. (2019). "RESEARCH AND DESIGN OF GRID-CONNECTED INVERTER IN PHOTOVOLTAIC SYSTEM WITH SVPWM TECHNIQUE." *International Journal of Engineering Technologies and Management Research*, 6(11), 18-31. DOI: <https://doi.org/10.29121/ijetmr.v6.i11.2019.4600>.

1. Introduction

Recently, the proportion of renewable energy resources, especially solar power energy, in total electricity generation is growing rapidly across many countries. Photovoltaic (PV), the mainstream solar power technology globally, generates direct current (DC) electricity. To convert this DC power to alternative current (AC) electricity, PV systems utilize a component called the inverter [1]. An inverter is a type of push pull converter that ensures the conversion of variable DC output of a PV solar panel into a utility frequency AC. The power supply generates DC, which is then put through an inverter with transistors to alter input and output signals of the current and produce output waveforms of AC power. The output voltage and amplifier is commonly controlled by inverters with Pulse Width Modulation technology.

Pulse Width Modulation (PWM) is one of the key controlling techniques in power electronics field. This technology is widely used in industrial applications that require high efficiency. PWM techniques frequently used in three phase voltage source inverters include the Sine Pulse Width Modulation (SPWM), Third Harmonic Injection Pulse Width Modulation (THIPWM), and Space Vector Pulse Width Modulation (SVPWM) [2].

In fact, SPWM is the very simple and commonly used controlling strategy in analogue circuit. However, it has some disadvantages such as high total harmonic distortion (THD), low switching frequency, and attenuation of the wanted fundamental component of the waveform. SPWM technique is compatible with both digital and analogue systems with applicable DC voltage of $0,5V_{DC}$. As a result, another controlling method should be utilized to accommodate the DC busbar. The technique, called Space Vector Modulation, is developed from the vector theory to figure out the method of modulating the sine-triangle carrier with better harmonic content and easier to control in digital circuits. The objective of any modulation technique is to obtain the output AC with fundamental component at peak and minimal harmonic distortion. As the voltage of DC busbar was wasted, the application and development of new controlling strategies to increase efficiency and reduce harmonic distortion for power inverter.

This paper considered the application of SVPWM controlling method to construct the voltage and amplifier specifications of SVPWM inverter. Synchronization process between the inverter and electricity grid is performed in phase-locked loop mechanism (PLL). After discussing theories and research methods, the paper will simulate the algorithm to evaluate the practical applications.

2. Space Vector Pulse Width Modulation Algorithm

Space Vector Modulation (SVM) is a modulation technique utilizing digital computation. This method could produce highly accurate AC output and be executed easily on modern digital circuits.

In a voltage source setting, a three phase current could be represented as a space vector with 3 components: $\mathbf{u} = (u_A, u_B, u_C)$ or $\mathbf{i} = (i_A, i_B, i_C)$, generally described as $\mathbf{X} = (X_a, X_b, X_c)$. This notion is not convenient as each vector is illustrated by 3 coordinate axes. In other words, a 3-axis coordinate system is constructed to plot the vectors. The Clarke transformation [3,9] is employed to transform a natural three-phase coordinate system into a stationary two-phase reference frame, facilitating the presentation of space vectors in normal setting. To simplify the model, vectors could be represented as bold and undercapitalized character (for example, \mathbf{u} , \mathbf{i} implies voltage vector and current vector). Using Clarke transformation, in any three phase system, voltage or current is depicted via a vector on a $0\alpha\beta$ plane as followed:

$$\mathbf{u} = 2/3 (u_A + au_B + a^2u_C) \quad (1)$$

In which, $a = e^{j2\pi/3} = -0,5 + j0,5.(3)^{1/2}$;

Based on equation (1): \mathbf{u} is a complex number, composed of the real part and the imaginary part, plotted on the complex coordinate system $0\alpha\beta$ as being followed:

$$\mathbf{u} = u_\alpha + ju_\beta \quad (2)$$

In which:

$$\begin{aligned}
 u_a &= \frac{2}{3} u_A - \frac{1}{2} u_B - \frac{1}{2} u_C \\
 u_b &= \frac{2}{3} \frac{\sqrt{3}}{2} u_B - \frac{\sqrt{3}}{2} u_C
 \end{aligned}
 \tag{3}$$

If u_A, u_B, u_C is a three-phase voltage source so that:

$$\begin{aligned}
 u_A &= U_m \cos(\omega t); \\
 u_B &= U_m \cos\left(\omega t - \frac{2\pi}{3}\right); \\
 u_C &= U_m \cos\left(\omega t + \frac{2\pi}{3}\right),
 \end{aligned}
 \tag{4}$$

In which, U_m denotes voltage variation, $\omega = 2\pi f$ denotes the angle of the space vector, t denotes time.

As a result, vector \mathbf{u} becomes:

$$\mathbf{u} = U_m \cdot e^{j(\omega t)}
 \tag{5}$$

This means on the $0\alpha\beta$ coordinates, \mathbf{u} is a vector with length equal to the amplitude of the phase voltages, orbiting around the origin of the coordinates axis at an constant angular rate of ω . Current vector is similarly identified using equation (1) or equation (3) for components of the current i_A, i_B, i_C .

In the three-phase voltage source inverter, as being illustrated in Figure 1, the power switches shall follow certain restriction rules. The constraints imposed in this system are that the input lines must never be shorted and the output current must always be continuous.

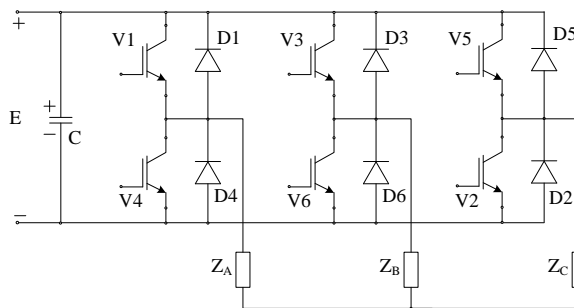


Figure 1: Three-phase inverter diagram [4]

Explanation: Do not short circuit the input DC, as it will generate a large current, damaging the switches. Do not open the output phase circuit because the AC circuit has inductance, sudden change of current will lead to over voltage. Moreover, when the control valve does not connect a certain output phase to the (+) or (-) busbar of the DC source, the current may still have to flow through the diodes, resulting in an output voltage that is dependent on the load, inversely. The flow

is no longer as inverted as desired. Restricted by these rules, a voltage source inverter can assume only eight distinctive topologies, as shown in Table 1 [5].

Table 1: Table of valve states and status vectors

No.	Valve	u_A	u_B	u_C	u
0	V2, V4, V6	0	0	0	0
1	V6, V1, V2	$2/3E$	$-1/3E$	$-1/3E$	$2/3Ee^{-j0}$
2	V1, V2, V3	$1/3E$	$1/3E$	$-2/3E$	$2/3Ee^{j\pi/3}$
3	V2, V3, V4	$-1/3E$	$2/3E$	$-1/3E$	$2/3Ee^{j2\pi/3}$
4	V3, V4, V5	$-2/3E$	$1/3E$	$1/3E$	$2/3Ee^{-j\pi}$
5	V4, V5, V6	$-1/3E$	$-1/3E$	$2/3E$	$2/3Ee^{-j2\pi/3}$
6	V5, V6, V1	$1/3E$	$-2/3E$	$1/3E$	$2/3Ee^{-j\pi/3}$
7	V1, V3, V5	0	0	0	0

Each of eight switch combinations determine corresponding phase voltage configurations. Calculating space vector u with equation (1), as being illustrated in the final column of Table 1. Power switch numbered 1 to 6 is represented by six vectors, namely u_1 to u_6 . The rotation angle of space vectors is 60-degree, plotted on $0\alpha\beta$ plane as in Figure 2. The tips of these vectors form a regular hexagon. We define the area enclosed by two adjacent vectors, within the hexagon, as a sector. Thus there are six sectors numbered I to VI. Two vectors corresponding to the power switch status of V2, V4, V6 loaded short circuit on (-) DC busbar. When power switch V1, V3, V5 is open, loading the short circuit to the (+) DC busbar. These two vectors produce zero output voltage, denoted as zero switching states u_0 and u_7 on vector coordinate [6]. The switching of the power valves in phases of the inverter generates a load phase voltage with its space vector changing over the hexagon.

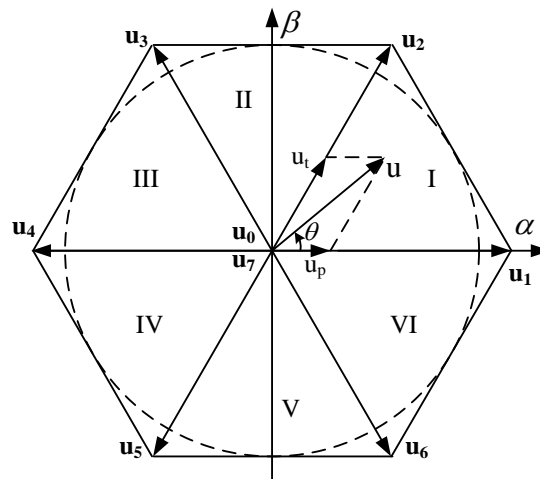


Figure 2: Space vector, status vector, and sector

For voltage source inverter ($2^3 = 8$), power switch is formed to match with 8 voltage vectors, which in turn shape the output voltage as indicated in Table 2 [7]. The mathematical equation to describe PWD technique could be found below. Three-phase voltages could be transformed to two-phase voltages via Clarke transformation.

Table 2: Table of valve states and status vectors

Voltage Vectors	Switching Vectors			Line to neutral voltage			Line to line voltage		
	a	b	c	u_{an}	u_{bn}	u_{cn}	u_{ab}	u_{bc}	u_{ca}
\vec{u}_0	0	0	0	0	0	0	0	0	0
\vec{u}_1	1	0	0	2/3	-1/3	-1/3	1	0	-1
\vec{u}_2	1	1	0	1/3	1/3	-2/3	0	1	-1
\vec{u}_3	0	1	0	-1/3	2/3	-1/3	-1	1	0
\vec{u}_4	0	1	1	-2/3	1/3	1/3	-1	0	1
\vec{u}_5	0	0	1	-1/3	-1/3	2/3	0	-1	1
\vec{u}_6	1	0	1	1/3	-2/3	1/3	1	-1	0
\vec{u}_7	1	1	1	0	0	0	0	0	0

3. Results and Discussions

The results section should provide details of all of the experiments that are required to support the conclusions of the paper. The section may be divided into subsections, each with a concise subheading.

It is advised that this section be written in past tense. It is a good idea to rely on charts, graphs, and tables to present the information. This way, the author is not tempted to discuss any conclusions derived from the study. The charts, graphs, and table should be clearly labeled and should include captions that outline the results without drawing any conclusions. A description of statistical tests as it relates to the results should be included.

A PV system is constructed with a three-phase grid-connected inverter as being illustrated in Figure 3. The output of PV cells are transmitted through a filter to a DC/DC Boost converter to perform the maximum power point tracking algorithms. The output voltage of DC/DC converter is then channeled to DC link before reaching the three-phase grid-connected inverter (PV inverter). To control the quality of electricity connecting to the grid, AC output of the PV inverter is linked with an output filter. This filter consists of an inductance in series with the inverter to mitigate total harmonic distortion before connecting the output AC with the grid. Additionally, system configuration uses a three-phase voltage sources to separate the filtered PV current and the grid.

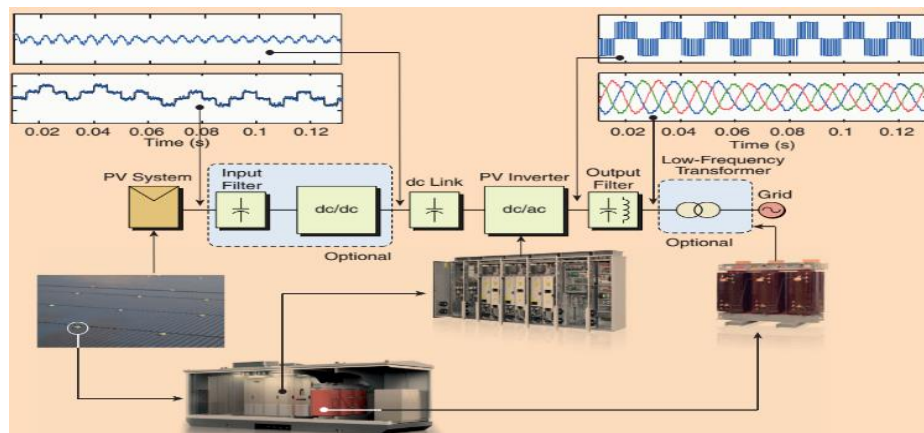


Figure 3: Components of PV system using three-phase grid-connected inverter.

3.1. DC/DC Converter

The type of DC/DC converter used in PV system is the Boost Converter (or step-up converter) [8] – Fig 4. The input signal from PV cells has a voltage of U_{PV} . The output signal U_{DC} of the Boost converter then becomes the input signal of the PV Inverter. During the voltage conversion process, maximum power point tracking (MPPT) algorithm is utilized.

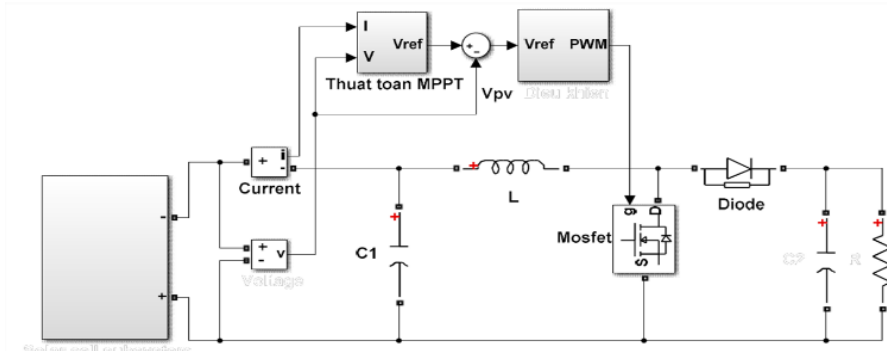


Figure 4: Boost Converter outline

In this research, we applied MPPT chaos optimization search and Perturb and Observer (P&O) algorithms to control the step-up DC voltage process for the simplicity and ease-to-use of these schemes [6]. MPPT algorithm tracks the cyclic rise and fall of voltage to find the maximum power operating point. If the variation of the voltage causes the power to increase, the subsequent variation will remain the same or reverse. Conversely, if the variation causes a decrease in capacity, the subsequent variation will tend to change in reverse. When the maximum power operating point is determined on the performance curve, the voltage variation will fluctuate around the highest power working point (Figure 5). Voltage variances cause power losses in the PV system, especially when weather conditions change slowly or stabilize. This technical issue can be solved by adjusting the order flow in the P&O algorithm to compare parameters in two previous cycles.

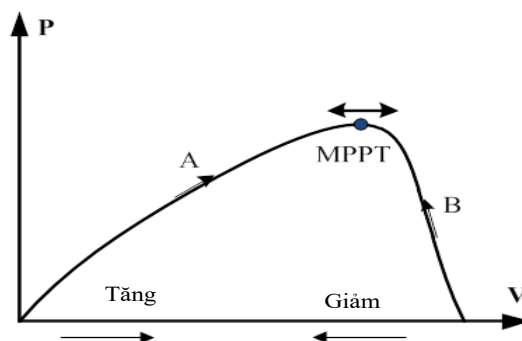


Figure 5: P&O algorithm to track MPP

P&O algorithm performs notably well under the circumstance that involve significant changes in weather conditions, allowing for incremental adjustment of MPPT in short time. Nevertheless, this algorithm remains some disadvantages such as: certain oscillation exists around the maximum power point; and the exiting oscillation around the MPP causes certain power loss. Within the scope of the paper, this algorithm satisfied designated requirements.

3.2. DC/AC Inverter

The structure of three phase grid-connected inverter is illustrated as a circuit structure in Fig. 6 and as a single-line diagram of the inverter in Fig. 7. Key components include: the converter, low-pass filter $R_f C_f$ (Filter) to minimize grid-current harmonics injected by grid-connected converters, the inductance L with an LD sensor and the RD resistor is used to accommodate the difference in voltage between the grid and the inverter output as well as to smooth current, transformers and switches [9]. Within the scope of the paper, the model has a modest power of 5kW, so capacitors can be omitted.

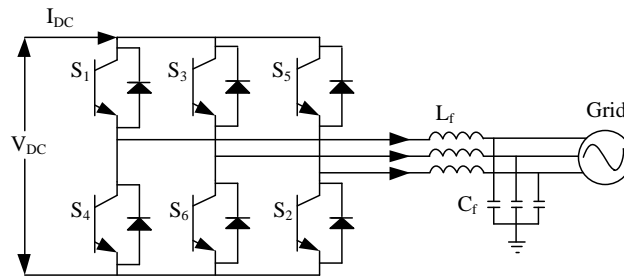


Figure 6: Representation of the three-phase grid connected inverter

Accordingly, Fig.8 represents simulation diagram of the constructed PV system. In this system, 5kWp power ratings of PV cells and a low voltage grid of 400V are selected as parameters.

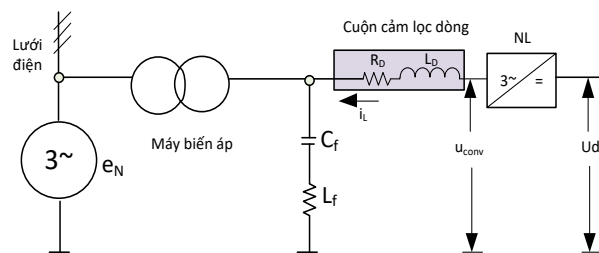


Figure 7: How grid-connect inverter works

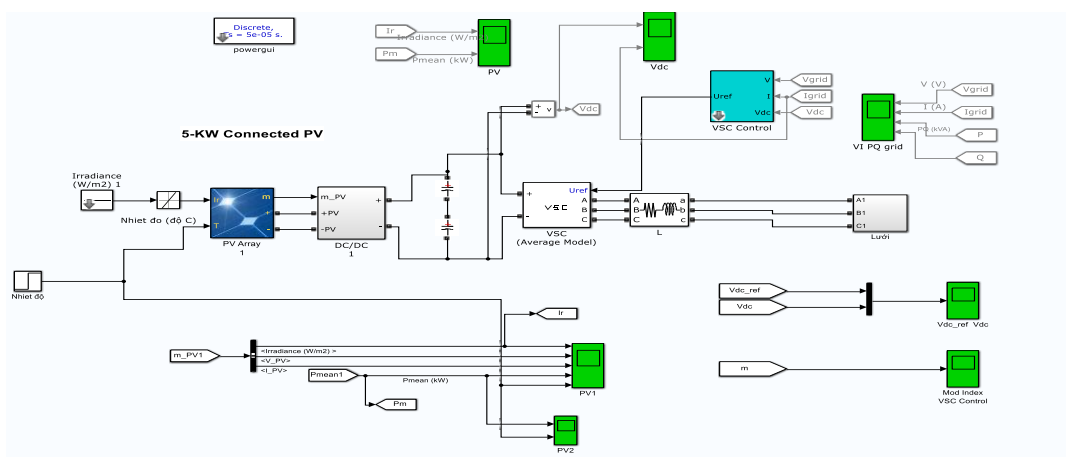


Figure 8: Simulation of grid-connected 5kWp PV system

3.3. Key Modules in Matlab Simulation

PV Cells Module

The PV array consists of 4 parallel PV series. Each series is formed by 4 PV cells, with the power of each PV cell reaches 315W – Fig.9. PV cells produce direct current. In this module, voltage change V_{DC} is treated as a parameter in simulation.

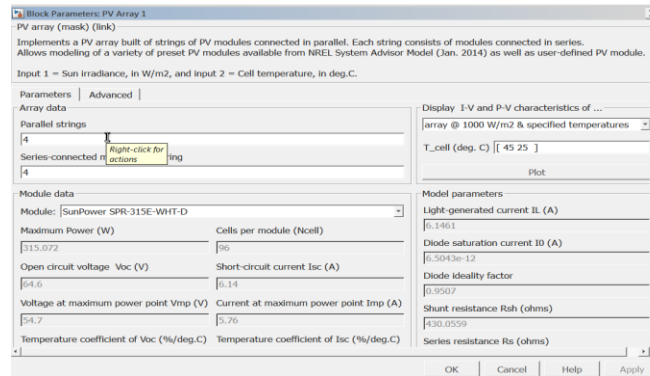


Figure 9: Configurations of PV array

DC/DC module (DC-DC Boost converter)

Boost Converter, or step-up voltage converter, elevates input voltage to produce higher output voltage (as being simulated in Fig.10).

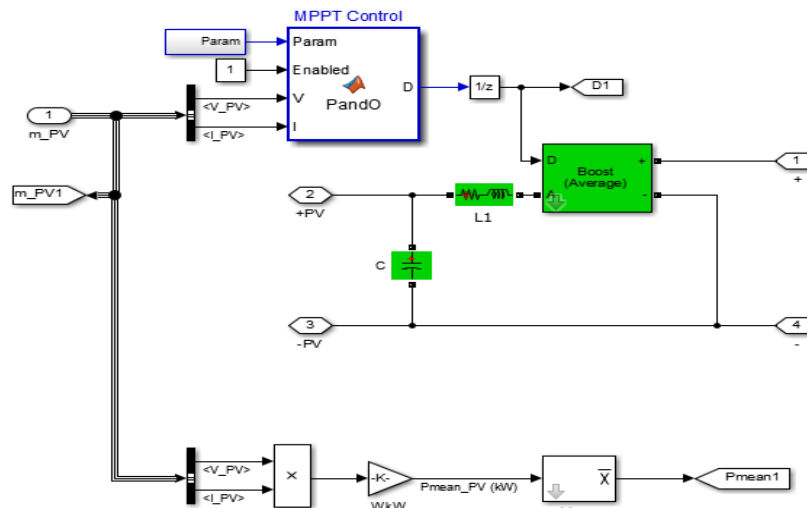


Figure 10: DC/DC converter diagram

The circuit consists of two semiconductor switches (a diode and a transistor) and a coil L for energy-accumulation, a capacitor C, and lastly a load R. The P&O algorithm is used for MPPT as mentioned in previous sections.

Voltage-sourced converters (VSC) module

This is the three-phase voltage-sourced inverter designed with SVPWM scheme as being presented in Section 1.

VSC Control module

A microcontroller signals the activation of high power transistors called IGBTs through pulse width modulation. By controlling which IGBTs are conducting through the 3-phase load, an alternating current is produced (Fig.11).

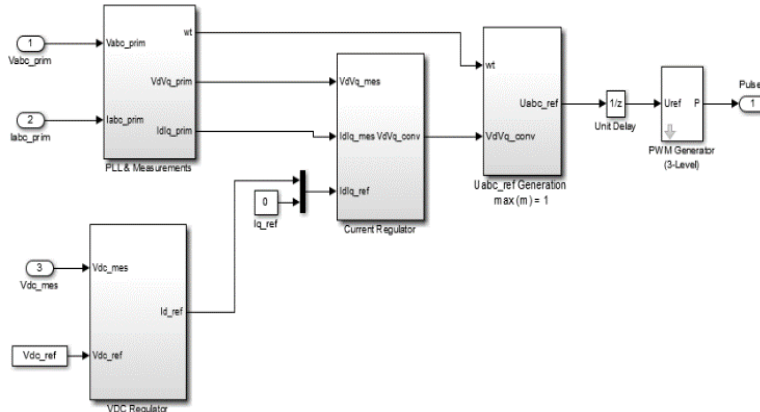


Figure 11: Control module diagram illustrated in Simulink

In the power transmitting process, DC bus voltage shall be stabilized, triggering the charging or discharging reactions on the capacitor. As a result, the PV system generates reactive power into the grid. To diminish this reactive power, on current control (q-axis), we set the value $i_{q_ref} = 0$ to make the value of reactive power equals to zero according to equation (4).

PLL & Measurement module

The input of this module is power and voltage signals generated by DC-AC inverter. At this stage, current and voltage vectors is converted from abc plane to dq0 reference frame via the Park transform to extract the instantaneous angle θ . The PV produces DC, which must be connected to AC grid. Thus, control for synchronization process is a crucial system component. The synchronization technique used in three phase inverter is phase-locked-loop (PLL). PLL unit is set to find the phase angle that match the mid phase of both DC side and AC side, as shown in Fig 12. Voltage regulator unit generates signal I_{d_ref} simultaneously through a measured DC voltage (V_{dc_mes}) and set voltage V_{dc_ref} to maintain the power factor $I_{q_ref} = 0$.

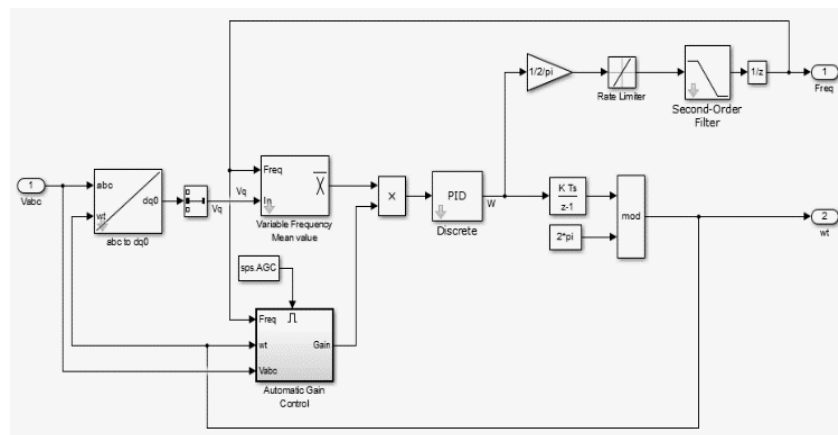


Figure 12: Simulation of PLL

Current regulator module: Basing on voltage value V_{dq_prim} , I_{dq_prim} and current value I_{dq_ref} are transformed into signal U_{dq_conv} . Voltage U_d and U_q obtained from the output of the current controller are calculated to find out set voltage signal U_{ref_abc} with suitable parameter of $U_{abc_refgeneration}$. This set voltage will be transmitted through SVPWM to generate signals controlling the output voltage of the inverter. The output of the three-phase inverter will flow through LC filter and transformer to filter high-order harmonics distortion and separate PV systems and grids.

Transformer module

The objective of this module is to accelerate voltage and separate PV system and the grid. A transformer with 5kVA power and 0,23/0,4kV voltage helps separate PV system and the grid. At the same time, this module triggers voltage from 0,23 kV to 0,4kV to facilitate the connection of PV current to low voltage electricity grid.

Measurement module

Measurement module (Fig 13) displays system’s parameter, such as reverse current source E; grid U, current I, active capacity P and resistance Q; U_{dc} ; I_d , I_q , etc.

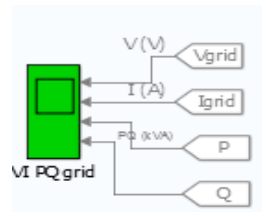


Figure 13: The display of voltage, current, P, Q on grid side

Control parameters

Table 3: Control parameters

Control units	K_p	K_i
Control unit for DC voltage	20	100
Control unit for current (dq)	0.015	1

Analyze and evaluate simulated results

- Effect of radiation intensity on generating power of PV system

Simulated results illustrated from Fig 14 to Fig 18 show that as light intensity changes, output capacity of PV system varies significantly. Output voltage of PV cells is around 200V. To ensure maximal power of generating source, MPPT algorithm shall be implemented.

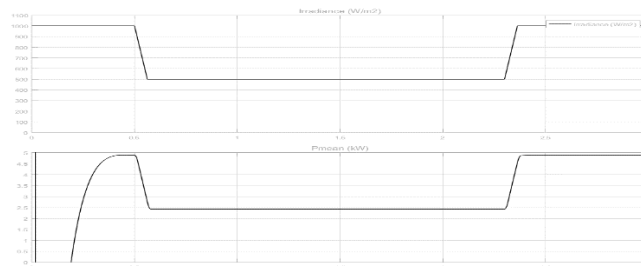


Figure 14: Power of current supplied to the grid with high intensity in 35°C condition

Output voltage of DC/DC converter is the set value for DC controller U_{DC} . Simulation results show that power of output DC current is also sensitive to light intensity. Intermediate DC voltage is quite stable when the system is set in a certain stage, indicating the balanced DC – DC converting process. The quality of the electricity injected into the grid (measured after the transformer) is good, illustrated by the analysis of current and harmonic form. Results of current simulation on the q-axis show that the current on the q-axis has been controlled to 0 after 1.5 seconds; in other words, reactive power has been controlled to zero.

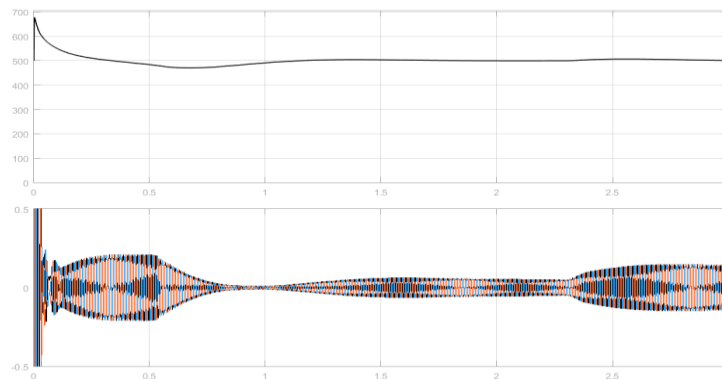


Figure 15: DC voltage on capacitor and electric form supplied to grid (after transformer)

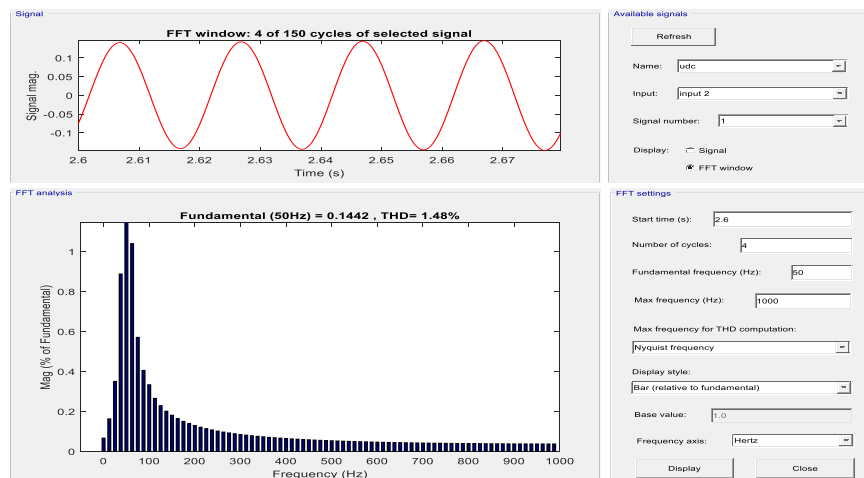


Figure 16: Harmonic distortion of current supplied to grid at $t = 2.6s$

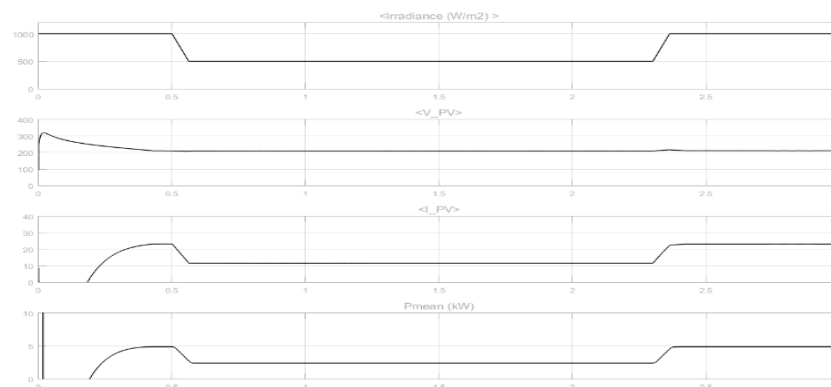


Figure 17: Output voltage, current, and power of PV system at different levels of light intensity

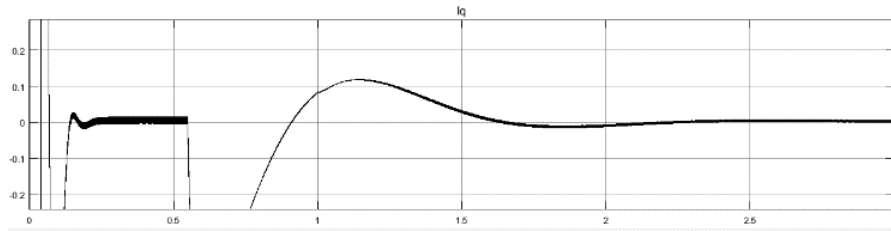


Figure 18: Value of current supplied to grid on q axis

Effects of temperature on generated power of PV system

PV system could be operated between -40°C and 85°C . The external temperature usually ranges from 10°C to 40°C . However, as PV cells are exposed to sunlight for a long-term period, the operating temperature of PV system will change. We will consider the influence of temperature on generating power of PV system at a constant light intensity I_r : $500\text{W}/\text{m}^2$ (depicted from Fig 19 to Fig 23).

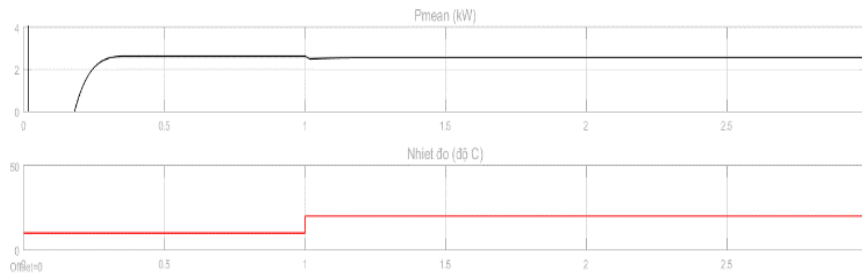


Figure 19: Power variance as temperate increases from 10°C to 20°C

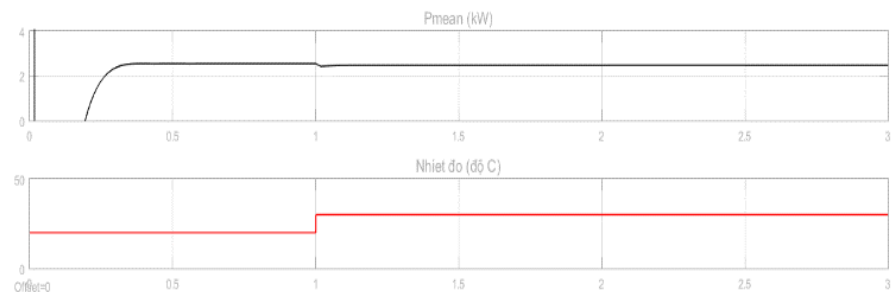


Figure 20: Power variance as temperate increases from 20°C to 30°C

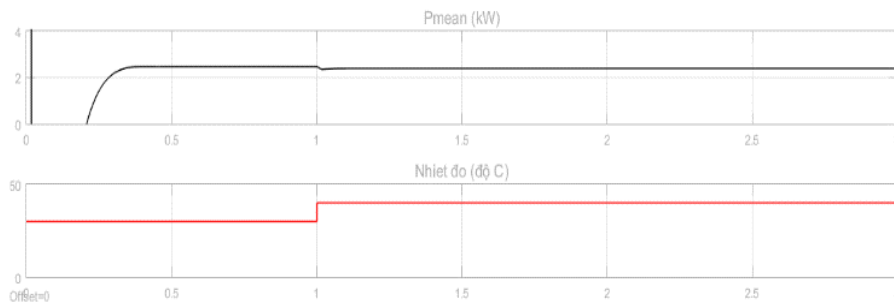


Figure 21: Power variance as temperate increases from 30°C to 40°C

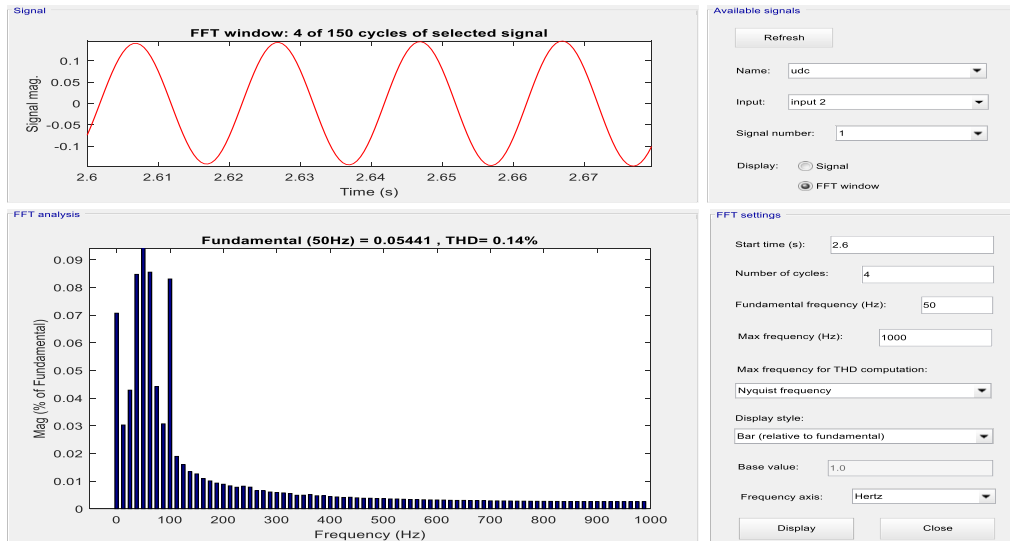


Figure 22: Harmonic distortion of current supplied to grid at time $t = 2,6s$ and temperature of $30^{\circ}C$

Remarks: As the external environment changes in temperature, output of PV system changes. The effect is not as markedly as in the case of changes in light intensity. In this senerio, the quality of the harmonics injected into the grid remains consistent with the results of harmonic analysis in Figure 3.45 and Figure 3.46.

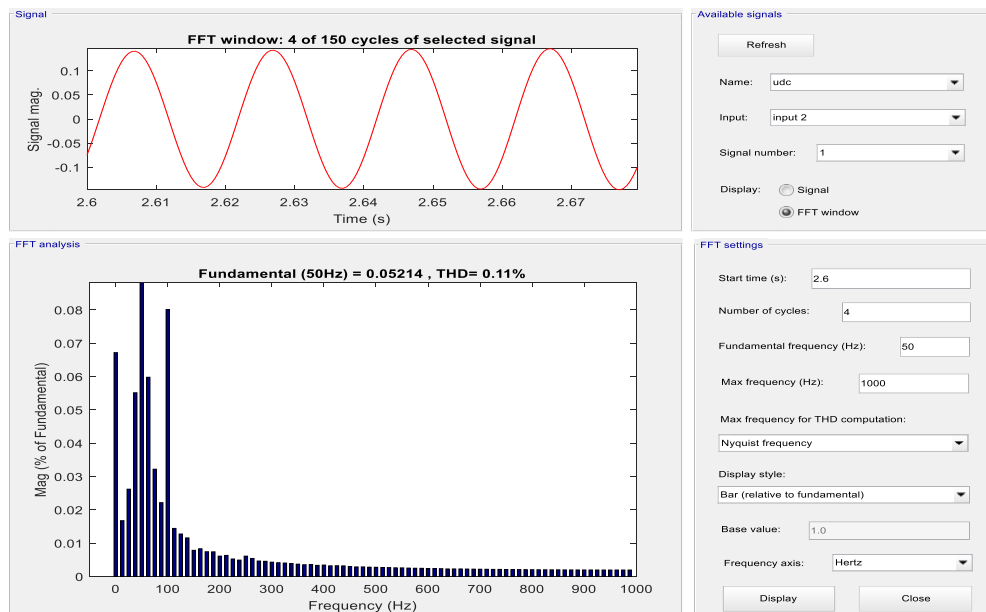


Figure 23: Harmonic distorion analysis of current supplied to grid at $t = 2,6s$ and temperature of $40^{\circ}C$

4. Conclusions

This paper proposed a framework design for three-phase grid-connected inverter using SVPWM technique. Simulated results under various grid connected scenarios indicate the successful application of space vector modulation in the proposed model.

Simulated results show that SVPWM provides enhanced baseline output with better quality, comparing to the results in the previous study [6]. The simulated model produced lower THD value than other PWM techniques. The efficiency of the conversion process is improved. The maximum voltage amplitude of the SVPWM method increases by about 90.6% compared to the SPWM method.

This paper successfully set up the control mechanism for the simulation inverter. Control loops for current and intermediate DC voltage are tested and analyzed. The voltage-sourced inverter models have physical and systematic application. The simulation shows that the SVPWM inverter used in the grid-connected PV system delivered ample results. Further practical application could be explored to enhance the efficiency of PV systems.

Acknowledgements

This paper is developed as a component of the study “Research, Design and Manufacture of Highly Efficient Inverter Connected to Distribution Grid for Solar PV System” Code: VAST07.04/18-19. The authors specially thank the Vietnam Academy of Science and Technology, Institute of Energy Science for providing fund for the study.

References

- [1] Tang Binwei; Yuan Tiejiang (2012); Simulation Models for Photovoltaic and Grid-Connected Simulation Based on PSCAD 2012(21)
- [2] Zamre Abd Ghani, M. A. Hannan, Azah Mohamed, Subiyanto Subiyanto (2011); Three-Phase Photovoltaic Grid-Connected Inverter using dSPACE DS1104 Platform. IEEE PEDS, 2011,12. 447-451.
- [3] Marian P. Kazmierkowski; R. Krishnan (2012); Frede Blaabjerg; “Control in Power Electronics”, Elsevier Science.
- [4] Trần Quang Thọ (2017); Điều khiển bộ nghịch lưu nối lưới trong mạng điện phân phối. Đại học Sư phạm Kỹ thuật Tp. Hồ Chí Minh, 2017.
- [5] M. P. Kazmierkowski and L. Malesani (1998); Current control techniques for three-phase voltage-source pwm converters: a survey. Industrial Electronics, IEEE Transactions on, vol. 45, No. 5, pp. 691–703, 1998.
- [6] Quang, N.P and Dittrich, J. (2012), "Vector control of three phase AC machine– System Development in the Practice”, Springer, Berlin – Heidelberg 2008
- [7] S. Thirupathi, Mrs.S.Devi (2014); A Novel Voltage Control Strategy for Three Phase Grid Connected System with Distributed Generation Inverters. International Journal of Innovative Research in Science, Engineering and Technology, 2014, 2(3)
- [8] Marian P. Kazmierkowski; R. Krishnan (2012); Frede Blaabjerg; “Control in Power Electronics”, Elsevier Science.

*Corresponding author.

E-mail address: minhnguyenduc.ies@ gmail.com